Diverse Responses of Upper Ocean Temperatures to Chlorophyll-Induced Solar Absorption Across Different Coastal Upwelling Regions

Siyu Meng[1,2] [ID], **Benjamin G. M. Webber**[1,2] [ID], **David P. Stevens**[1,3] [ID], **Manoj Joshi**[1,2] [ID], **Julien Palmieri**[4] [ID], and **Andrew Yool**[4] [ID]

[1]Centre for Ocean and Atmospheric Sciences, University of East Anglia, Norwich, UK, [2]Climatic Research Unit, School of Environmental Sciences, University of East Anglia, Norwich, UK, [3]School of Mathematics, University of East Anglia, Norwich, UK, [4]National Oceanography Centre, Southampton, UK

Abstract Chlorophyll in phytoplankton absorbs solar radiation (SR) and affects the thermal structure and dynamics within upwelling regions. However, research on this process across global-scale coastal upwelling systems is still lacking. Here, we use a coupled ocean-biogeochemical model to investigate differing responses to chlorophyll-induced solar absorption between Pacific and Atlantic coastal upwelling regions. Chlorophyll-induced solar absorption leads to colder Pacific coastal upwelling but warmer Atlantic coastal upwelling. In the Pacific, the shading effect of the surface chlorophyll maximum leads to colder subsurface water, which is then upwelled, contributing to cooling. The more stratified upper ocean leads to shallower mixed layer depth, intensifying offshore transport and upwelling. In the Atlantic, the absorption of SR by the subsurface chlorophyll maximum causes warmer and weaker upwelling. The processes described, in turn, trigger positive feedback to ocean biogeochemistry and potentially interact with climate dynamics, underscoring the necessity to incorporate them into Earth system models.

Plain Language Summary Chlorophyll and related pigments in phytoplankton play a key role in absorbing solar radiation and regulating ocean temperatures. In some coastal upwelling regions along the eastern boundaries of oceans, where chlorophyll concentrations are high, studies have suggested that the solar heat absorbed by chlorophyll can influence the temperatures and strength of upwelling. However, there is no study focusing on this process across global coastal upwelling zones. Here, we use computer simulations of ocean and phytoplankton to explore the effects of chlorophyll-induced solar absorption on upwelling temperatures and strength on a global scale. Our study suggests that this effect varies between Pacific and Atlantic coastal upwelling regions due to their different spatial distributions of chlorophyll: surface chlorophyll in the Pacific warms the water after it has risen to the surface and as it is flowing offshore, while subsurface chlorophyll in the Atlantic warms the water before it rises to the surface. As a result, chlorophyll-induced solar absorption leads to colder and stronger coastal upwelling in Pacific but warmer and weaker upwelling in Atlantic. Given the limited consideration of this process in previous studies, we emphasize the importance of incorporating it, along with regional differences, into future simulations.

1. Introduction

Phytoplankton, the primary photosynthetic organisms in the ocean, plays a crucial role in regulating the vertical distribution of solar radiation (SR) through absorption by chlorophyll (Chl) and related pigments (Marlon et al., 1990; Morel, 1988). Previous research has established a connection between Chl-induced solar absorption and the thermal structure of the upper ocean, based on observations (Huan et al., 2021; Mercado & Gómez-Jakobsen, 2022), in situ data (Parida et al., 2022; Patil et al., 2023), and numerical models (Asselot et al., 2021; Park et al., 2014). For instance, SR absorption by Chl has been proposed as a significant contributor to the upper ocean heat balance in the open ocean, manifesting in the increase of upper ocean heating rate ranging from 2 to 20 W m^{-2} (Parida et al., 2022; Park et al., 2015; Timmermann & Jin, 2002). Thus, higher phytoplankton biomass generally leads to a warmer ocean surface layer and exerts a significant influence on global climate (Manizza et al., 2005, 2008). However, some state-of-the-art climate models, such as the UK Earth System Model (UKESM), still lack a realistic representation of this process, relying on a spatially constant Chl value for SR penetration calculations (Sellar et al., 2019). This constraint, along with the significant implications of Chl-

Resources: Benjamin G. M. Webber, Julien Palmieri, Andrew Yool
Software: Siyu Meng
Supervision: Benjamin G. M. Webber, David P. Stevens, Manoj Joshi
Validation: Siyu Meng, Benjamin G. M. Webber, David P. Stevens
Visualization: Siyu Meng
Writing – original draft: Siyu Meng
Writing – review & editing: Siyu Meng, Benjamin G. M. Webber, David P. Stevens, Manoj Joshi, Julien Palmieri
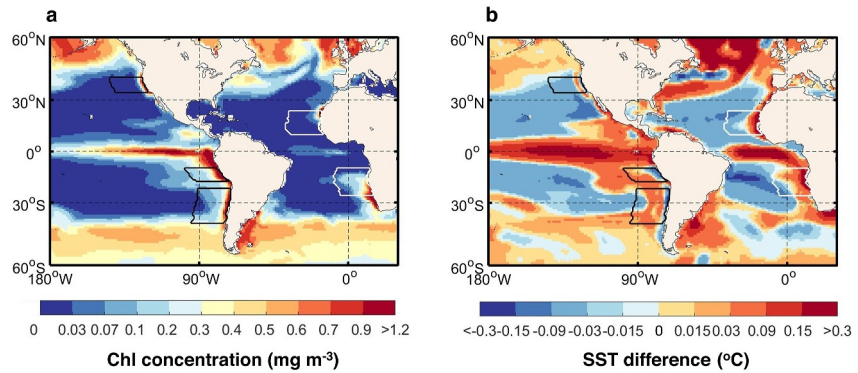
Figure 1. Response of sea surface temperature (SST) to Chl-induced solar absorption in coastal upwelling regions. (a) Distribution of surface Chl concentration in Case.MED. (b) SST difference of Case.MED minus Case.Con. Black lines indicate Region.Cold, denoting coastal areas exhibiting surface cooling induced by Chl, and white lines indicate Region. Warm, denoting coastal areas exhibiting surface warming induced by Chl.

induced solar absorption for ocean physics and climate processes, emphasizes the need for a comprehensive investigation into this biophysical interaction.

Solar radiation absorption by Chl has been suggested to impact the large-scale climate variability (Jochum et al., 2010; Tian et al., 2021; R. H. Zhang et al., 2019), and studies on this effect have mainly centered on the Pacific equatorial upwelling region, due to its potential feedbacks to the El Niño-Southern Oscillation (ENSO). For example, the variations in the upper ocean thermal structure induced by Chl-absorbed SR in the Pacific equatorial upwelling significantly influence the magnitude (Lengaigne et al., 2007) and asymmetry (Timmermann & Jin, 2002) of ENSO. However, the thermal structure in the coastal upwelling regions, situated along the eastern boundaries of mid-latitude ocean basins, can also influence the formation of stratocumulus clouds by changing the ocean-atmosphere fluxes of heat and moisture, and can thus indirectly impact tropical or broader climate (Richter, 2015; Wood, 2012). Hence, it is essential to understand the modification of Chl on the thermal structure of coastal upwelling, as it may exert a substantial impact on climate system.

Previous studies have explored the Chl-induced temperature variations within specific upwelling systems. As indicated by Echevin et al. (2021), increased surface Chl concentrations in the Peru upwelling can absorb more SR in the upper ocean, thereby limiting its penetration into the subsurface. This process leads to a cooling of the upper ocean, attributed to the subsurface cooling of source waters that are upwelled. Furthermore, Hernandez et al. (2017) suggests a comparable surface cooling impact by Chl in the Benguela and Canary upwelling systems. This cooling effect is associated with not only the redistribution of SR but also the modifications in horizontal ocean advection. However, Hernandez et al. (2017) uses an empirical parameterization (Morel & Berthon, 1989) to estimate a vertical profile of Chl from satellite-observed surface Chl, which introduces uncertainty into the vertical structure of SR absorption by Chl in the subsurface ocean.

While Chl-induced solar absorption has been associated with ocean thermal structure and dynamics in specific coastal upwelling regions, there remains a need for a comprehensive understanding and comparison of these processes across global coastal upwelling regions, using the same model and assumptions for each region. In this study, we use a global ocean model coupled with a biogeochemistry model to investigate the influence of Chl-induced solar absorption on upper ocean temperatures and dynamics in five coastal upwelling regions (Figure 1), with a specific focus on exploring the discrepancies between them.

2. Data and Methods

2.1. Model Description

Numerical experiments in this study make use of the Nucleus for European Modeling of the Ocean (NEMO) (Madec & NEMO team, 2016) ocean physics model coupled with the Model of Ecosystem Dynamics, nutrient Utilization, Sequestration and Acidification (MEDUSA) (Yool et al., 2013) marine biogeochemistry model. The model domain is approximately $1° \times 1°$ in horizontal resolution, with 75 vertical levels and an explicit nonlinear

free surface. In NEMO, SR absorption down the water column depends on the Chl concentration at each model level, using a three-waveband Red-Green-Blue (RGB) light scheme (Lengaigne et al., 2007; Morel, 1988). Operationally, the model permits this Chl concentration to be directly driven by MEDUSA or to be specified independently. In MEDUSA, the solar absorption is calculated separately from NEMO based on a two-waveband light scheme to represent the self-shading by phytoplankton within the water column (Yool et al., 2013). In Section 3.2, mixed layer depth (MLD) is used to explain the response of upwelling dynamics to Chl-induced solar absorption. Here, MLD is defined as the depth where the vertical profile of potential temperature decreases by 0.5°C relative to the near-surface temperature.

Here, the configuration of NEMO-MEDUSA has been made consistent with that of the UKESM1 (Sellar et al., 2019). UKESM is a fully coupled Earth system model that is built upon the HadGEM3-GC3.1 (Kuhlbrodt et al., 2018) physical climate model, adding interactive atmospheric chemistry and terrestrial and marine biogeochemistry (MEDUSA). HadGEM3-GC3.1 omits marine biogeochemistry, and instead utilizes a spatially uniform Chl value when calculating the absorption of downwelling radiation in the ocean. To remain consistent with HadGEM3-GC3.1, UKESM1 also uses this approach, despite MEDUSA including Chl dynamics. As a result, this may lead to unrealistic model behavior, especially in regions where MEDUSA's Chl differs significantly from this constant value. For example, where simulated Chl is much lower, as in the low productivity oligotrophic gyres (Dai et al., 2023), or much higher, as in the highly productive upwelling regions (Ferreira et al., 2021). Consequently, by contrasting model behavior when this constant value is used with that when MEDUSA's dynamic Chl concentrations are used, this study aims to provide insights for future Earth system model development.

2.2. Case Settings

The two case simulations in this study only differ in the Chl inputs of the RGB scheme, the component for calculating solar absorption in NEMO. In the reference simulation (Case.Con), the SR penetration is based on a horizontally and vertically constant Chl concentration set to 0.1 mg m^{-3}, which is the default value in NEMO. In Case.MED, SR penetration depends on the time-varying output of Chl concentrations from MEDUSA. Both cases are forced at the ocean surface by identical atmospheric forcing, including SR, heat, freshwater and momentum fluxes, provided by version 2 forcing for coordinated ocean-ice reference experiments (CORE2) (Griffies et al., 2009).

2.3. Observational Data

Observed sea surface Chl concentration data is used to evaluate the model performance in Figure S1 in Supporting Information S1. Monthly mean Chl concentrations are derived from Moderate Resolution Imaging Spectroradiometer (MODIS) satellite data spanning 2005 to 2022 (NASA OBPG, 2022). For ease of computation, the raw data is interpolated to the model grids.

3. Results

3.1. Modifications of Chl-Induced Solar Absorption on Upper Ocean Temperatures in Coastal Upwelling Regions

Chl concentrations simulated by MEDUSA within global coastal upwelling regions consistently exceed 0.1 mg m^{-3}, the reference value to calculate SR penetration in Case.Con (Figure 1a). However, higher Chl levels exhibit a contrasting impact on sea surface temperatures (SSTs) between different coastal upwelling regions, producing a surface cooling in Pacific upwelling regions but a surface warming in Atlantic upwelling regions (Figure 1b).

To understand the different responses of SSTs to Chl between Pacific and Atlantic coastal upwelling regions, we have categorized global coastal upwelling regions (Chavez & Messié, 2009; Patti et al., 2008) into two zones: Region.Cold and Region.Warm (Figure 1). Region.Cold is defined as the coastal upwelling regions where the enhanced Chl-induced solar absorption leads to colder surface temperatures in Case.MED compared with Case.Con. These regions include California, Peru, and Chile upwelling zones in the Pacific ocean. Conversely, Region.Warm, situated along the eastern coasts of the Atlantic, experiences warmer surface temperatures due to enhanced Chl-induced solar absorption.
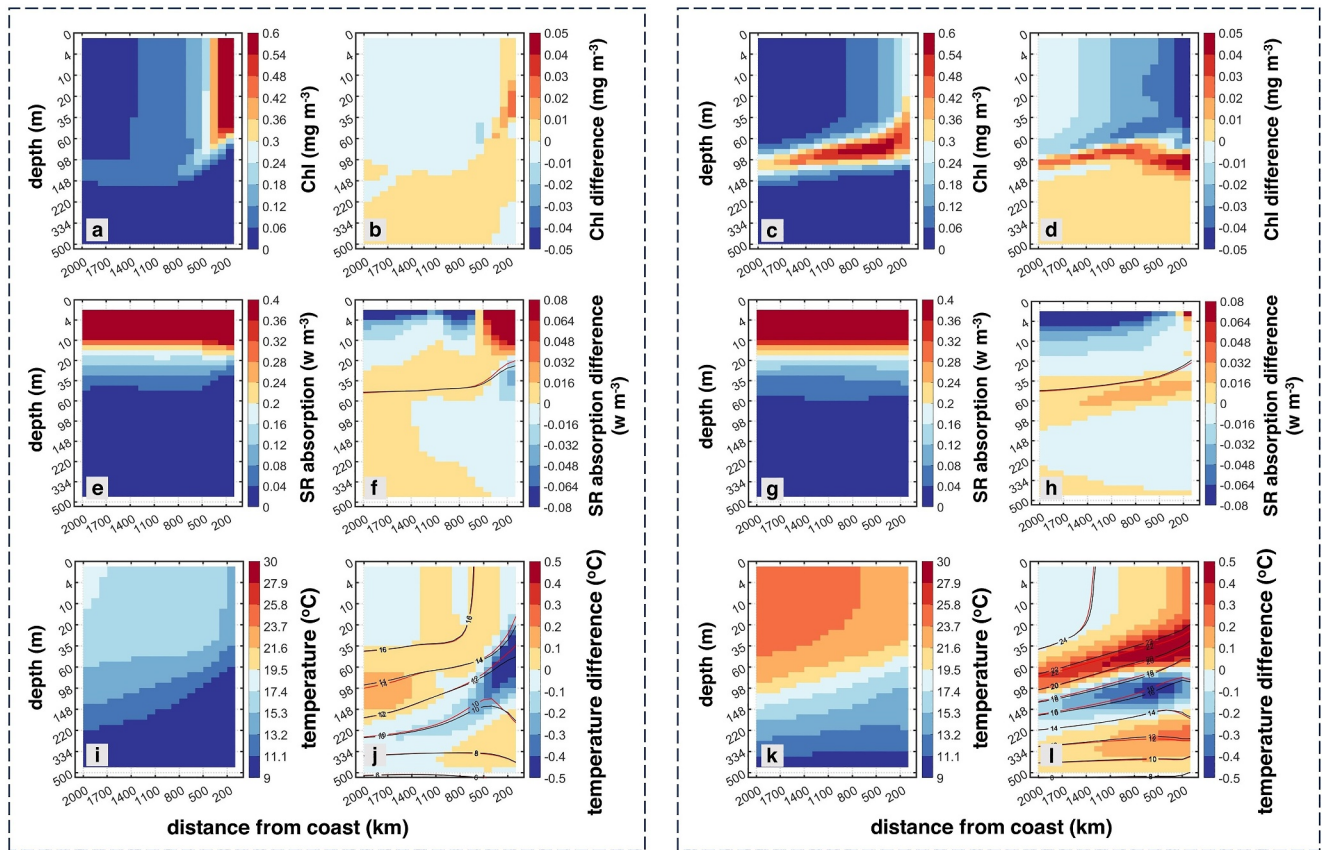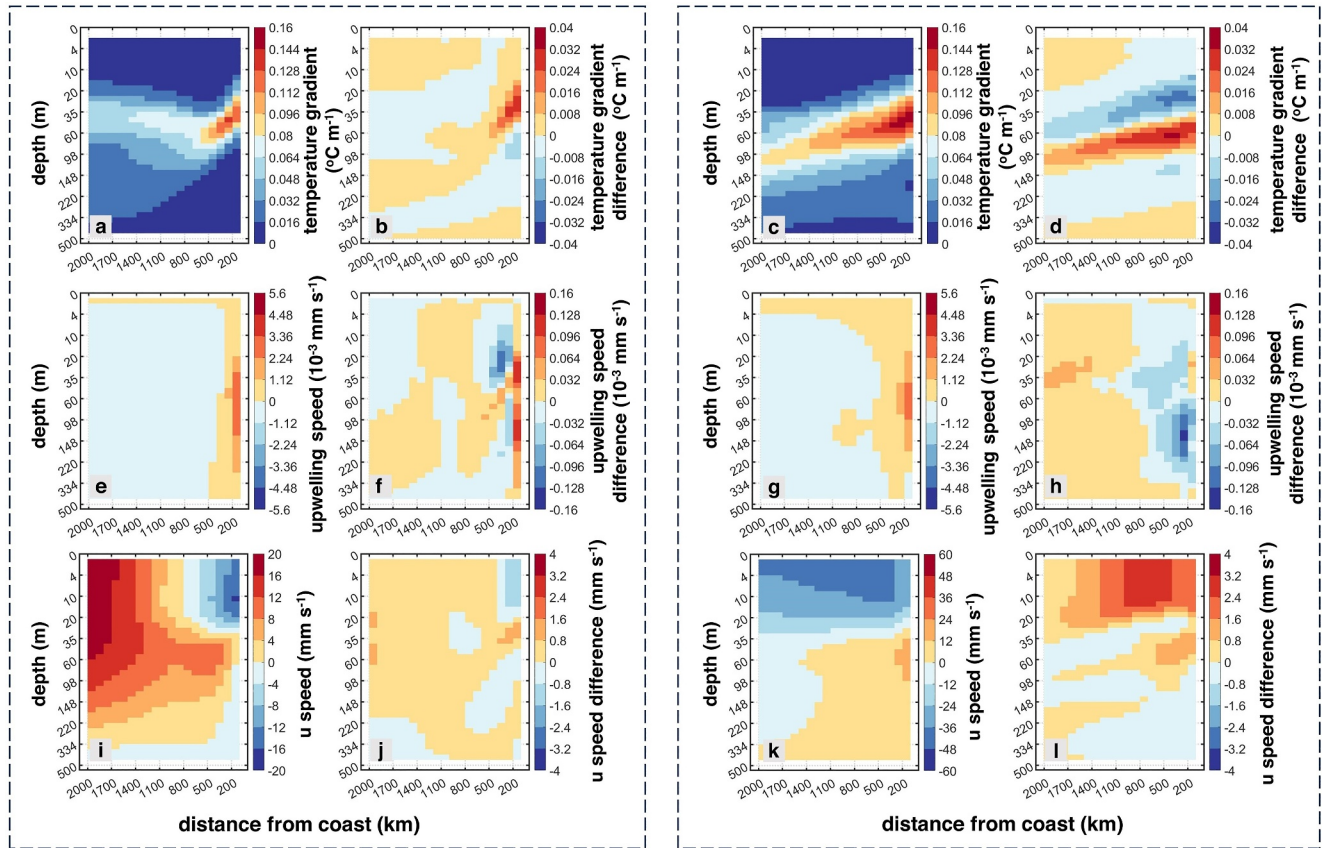
Figure 2. Mean cross-shore structures of Chl concentrations (a, c), solar radiation absorption per unit depth (e, g) and potential temperature (i, k) in Case.MED and their differences of Case.MED minus Case.Con (b, d, f, h, j, and l) in Region.Cold (left dashed box) and Region.Warm (right dashed box) as indicated in Figure 1. Red lines in panels (f) and (h) indicate the mixed layer depth (MLD) in Case.MED, and black lines indicate the MLD in Case.Con. Red lines in panels (j) and (l) indicate the isotherms in Case.MED, and black lines indicate the isotherms in Case.Con.

In Region.Cold, high near-surface Chl concentrations simulated by MEDUSA (Figure 2a) lead to increased absorption of SR within the upper 20 m depth (Figure 2f) in Case.MED. This, in turn, restricts the penetration of SR into the subsurface ocean (Figure 2f), resulting in subsurface cooling below 20 m depth (Figure 2j). Subsurface colder water is subsequently transported to the surface via upwelling (Figure 3e), while the solar heat accumulated in the near-surface ocean is transported away from the coast via horizontal advection (Figure 3i). This mechanism leads to the surface cooling within approximately 300 km of the coast within the upwelling regions and simultaneous warming farther offshore (Figure 1b).

In Region.Warm, the modification of the vertical distribution of SR by Chl is similar to that of Region.Cold, that is, more SR absorbed in the upper ocean and less penetration into the subsurface (Figure 2h). However, this effect is less pronounced in Region.Warm, primarily due to the lower Chl concentrations in the near-coast surface ocean (Figure 2c). Notably, within the range of 200–1,500 km away from the coast in Region.Warm, more SR is accumulated in the subsurface ocean (at around 60 m depth) (Figure 2h), driven by the presence of a subsurface Chl maximum (Figure 2c). As a result, additional solar heat is transported toward the coast at depth (Figure 3k) and then upwelled (Figure 3g), leading to an upper ocean warming in the coastal upwelling regions (Figure 2l).

3.2. Impacts of Chlorophyll-Induced Temperature Variations on Ocean Dynamics

Aligned with the differing temperature responses to Chl-induced solar absorption between the different upwelling regions, the subsequent effects on ocean dynamics differ and are described in this section. The wind forcing, acting as the atmospheric driver of coastal upwelling, remains constant in both cases. However, physical changes in the ocean resulting from Chl-induced solar absorption could potentially influence the offshore transport and thus the upwelling dynamics.

Figure 3. Mean cross-shore structures of vertical temperature gradient (a, c), upwelling speed (e, g) and eastward (u-ward) current speed (i, k) in Case.MED and their differences of Case.MED minus Case.Con (b, d, f, h, j, and l) in Region.Cold (left dashed box) and Region.Warm (right dashed box) as indicated in Figure 1.

In Region.Cold, the reduction in subsurface temperatures (20–140 m depth) resulting from the Chl shading effect intensifies the vertical stratification in the upper ocean (Figure 3b) and leads to a shallower MLD in Case.MED (Figure 2f). The change of MLD only has a small impact on the solar absorption within the mixed layer. However, based on the calculation of net offshore transport (Text S1 in Supporting Information S1) following Sweeney et al. (2005), a shallower MLD intensifies offshore geostrophic transport, which largely explains the stronger net offshore transport in the mixed layer in Case.MED (Figure S2a in Supporting Information S1). This leads to an intensified upwelling, peaking just below the enhanced offshore velocity anomalies (Figure 3j), to compensate the water transported away from the coast in the mixed layer (Figure 3f). Moreover, in Case.MED, the additional water transported away from the coast at the ocean surface is subsequently transported back to the coast through more pronounced downwelling between 200 and 500 km offshore, and subsurface coastward currents at around 60 m depth (Figures 3e–3j). This process enhances the existing mesoscale zonal overturning circulation in these upwelling regions, characterized by an "upward-offshore-downward-onshore" flow pattern (Figures 3f and 3j). The intensified upwelling near the coast contributes to cooling the near-coast water column, whereas enhanced downwelling farther offshore leads to the off-coast warming. This process, along with the Chl-induced redistribution of solar heat (Figure 2f), collectively contributes to the negative temperature anomalies in near-coast regions and positive temperature anomalies in off-coast regions (Figure 2j).

In Region.Warm, the less stratified upper ocean (above 60 m depth) leads to a deeper MLD in Case.MED (Figure 2h). This weakens the offshore transport (Figure 3l and Figure S2b in Supporting Information S1), resulting in a reduced upwelling speed (Figure 3h). The circulation anomalies (Figures 3h and 3l) are broadly opposite to those in Region.Cold, indicating a weakening of the zonal overturning circulation consistent with a slower offshore current.

4. Discussion and Conclusions

The responses of the thermal structure and dynamics to Chl-induced solar absorption vary between the Pacific and Atlantic coastal upwelling regions. In the Pacific coastal upwelling regions, increased Chl-induced solar absorption produces cooling in the near-coast areas but simultaneous warming farther offshore. This is in line with Echevin et al. (2021), who proposed a cooling impact of Chl-induced solar absorption in the near-coast Peru upwelling region. However, the maximum surface cooling reported in their study, up to 1°C, is larger than the 0.3°C in our study (Figure 1b). One possible reason is that the reference simulations of Echevin et al. (2021) are based on no Chl as opposed to 0.1 mg m^{-3} in our study, accentuating the Chl-induced cooling which is calculated based on the Chl differences between reference and experimental simulations. Additionally, Echevin et al. (2021) used a fine-resolution regional ocean model (10 km horizontal resolution), enabling a more accurate simulation of the fine structure of the cooling effect caused by near-coast high Chl concentrations (Hilt et al., 2020).

In the Atlantic coastal upwelling regions, solar heat absorbed by the subsurface Chl maximum is transported coastward by the subsurface eastward currents and then upwelled, resulting in an upper ocean warming (above 80 m) of the near-coast upwelling region. As a result of increased absorption of SR at a depth of 60–80 m, there is a reduction in the penetration of SR into the deeper ocean. Consequently, the negative anomaly of solar heat input below 80 m depth (as shown in Figure 2h) is trapped in the stratified deep ocean, leading to a cooling effect within 80–150 m depth (Figure 2l). This finding contrasts with Hernandez et al. (2017) who proposed a surface cooling caused by Chl-induced solar absorption in the Benguela and Canary upwelling systems. The difference might arise from the unrealistic vertical profile of Chl in their study, which was calculated by an empirical parameterization (Morel & Berthon, 1989) combined with satellite-observed surface Chl concentrations. This approach may not accurately capture the Chl-induced temperature change if the empirical parameterization only alters the distribution of SR within the mixed layer in response to varying Chl concentrations (see Figure 2 in Hernandez et al. (2017)), and it may fail to represent the warming effect induced by the Atlantic subsurface Chl maximum which is below the mixed layer (Figure 2h). Therefore, we emphasize the importance of simulating Chl vertical distribution especially relative to the mixed layer when evaluating the effect of Chl-induced solar absorption (Du et al., 2024; R. H. Zhang et al., 2018).

Furthermore, these results have been compared with the studies in equatorial upwelling regions. In the Pacific ocean, similar cooling responses to Chl-induced solar absorption are found in both coastal and equatorial upwelling regions, as supported by the majority of studies focused on equatorial upwelling (Shi et al., 2023; R. H. Zhang et al., 2019). This similarity is attributed to the redistribution of SR caused by Chl (less penetration into subsurface and then upwelled) and resultant stronger surface divergence and upwelling (Murtugudde et al., 2001; Shi et al., 2023). However, the cooling effect in the Pacific coastal upwelling regions is more pronounced due to the higher upwelling speed which can transport more of the colder water affected by the Chl shading effect (see Figure 2 in Shi et al. (2023)). In the Atlantic ocean, SST responses to Chl-induced solar absorption differ between coastal and equatorial upwelling regions due to varying dynamic and biogeochemical conditions. In equatorial upwelling regions, the variations in complex ocean currents induced by Chl result in negative feedback on SST (Murtugudde et al., 2001), while in coastal regions, more pronounced subsurface Chl maximum leads to positive feedback on SST (Figure S3 in Supporting Information S1).

We further assess the uncertainties in the results introduced by the methods used in this study. A comparison of surface Chl concentrations between modeling output and satellite observations (Figures S1a and S1b in Supporting Information S1) shows that the Chl distribution in the Pacific upwelling regions is well captured by MEDUSA, although it overestimates Chl concentrations in the Peru upwelling region. In Atlantic coastal upwelling regions within 10°S–10°N, MEDUSA exhibits a negative bias in surface Chl concentrations (Figure S1b in Supporting Information S1). Nevertheless, MEDUSA accurately reproduces the subsurface Chl maximum in this region, which is a key feature contributing to the Atlantic upwelling warming (Figure S3 in Supporting Information S1 and Yasunaka et al. (2022)). Due to the inaccurate simulation of nutrient availability in MEDUSA (Yool et al., 2021), the positive bias in surface Chl of Pacific coastal upwelling and negative bias in the Atlantic may exaggerate the findings of this study. However, the primary aim of this research is to understand the response of ocean physics to Chl-induced solar absorption, rather than to reproduce precisely the observed ocean conditions. Furthermore, the key results of this study are all statistically significant at the 95% level, based on a Student's *t*-test analysis of the anomalies (Figure S4 in Supporting Information S1).

The Chl-induced variations in upper ocean temperatures can further alter the ocean dynamics of upwelling regions. Following Sweeney et al. (2005), the net offshore transport, which governs upwelling strength, is determined by two components: Ekman transport and geostrophic transport (Text S1 in Supporting Information S1). The Ekman transport within the mixed layer remains consistent between the Case.MED and Case.Con simulations due to identical wind forcings in both cases. Therefore, changes in upwelling dynamics are governed by any variations in the geostrophic transport, in line with Ding et al. (2021) and Jing et al. (2023). In Pacific coastal upwelling regions, the enhanced stratification in the upper ocean associated with Chl-induced solar absorption leads to a shallower MLD. This intensifies the offshore geostrophic transport and can largely explain stronger net offshore transport in Case.MED (Figure S2a in Supporting Information S1). Finally, the intensification of offshore transport contributes to a stronger upwelling in the upper ocean (Figure 3f). The same mechanism produces the opposite response in Atlantic coastal upwelling regions due to the deeper MLD produced by the deep Chl maximum here (Figure S2b in Supporting Information S1).

However, the calculations of net offshore transport only provide an incomplete dynamical interpretation for coastal upwelling, as it may overlook the remote effects of larger-scale circulation, which is an important component in coastal upwelling systems (Lee et al., 2024). Hence, we present the difference of horizontal currents between two cases within coastal upwelling regions in Figure S5 in Supporting Information S1. In Pacific coastal upwelling regions, the horizontal currents in Case.MED show a 10% increase compared to Case.Con (Figures S5e and S5f in Supporting Information S1), attributed to stronger geostrophic transport, aligning with stronger offshore transport and upwelling caused by Chl-induced solar absorption (Figure 3f). However, in Atlantic upwelling regions, variations in ocean currents caused by Chl-induced solar absorption appear to be part of a broader pattern of surface current anomalies, likely correlated with other dynamical changes, such as equatorial currents and larger-scale circulations (Figures S5g and S5h in Supporting Information S1), although these must ultimately be driven by the difference in Chl between the two simulations. Therefore, future research should investigate both local and remote processes driven by changes in Chl-induced solar absorption and resultant impacts on ocean dynamics.

The variations in ocean dynamics caused by Chl-induced thermal structure change potentially feedback to the upper ocean temperatures (Figures 3e–3l). To quantify the relative contribution of changes in ocean currents on Chl-induced temperature variations, a heat budget analysis has been applied to Case.MED and Case.Con (Figure S6 in Supporting Information S1). The heat budget differences between the two cases align with our results, revealing a solar heating effect in the upper ocean but a cooling effect from the transport of colder subsurface water in Pacific coastal upwelling regions (Figures S6a–S6f in Supporting Information S1), and a warming effect in subsurface water of Atlantic coastal upwelling regions (Figure S6c in Supporting Information S1) which is then upwelled (Figures S6d and S6h in Supporting Information S1). We also conduct sensitivity tests by calculating the heat budget difference between Case.MED and Case.Con under the assumptions that either the ocean currents are kept constant or the temperatures are kept constant (Figure S7 in Supporting Information S1). Qualitatively, the heat budget difference patterns between the two cases align closely with those caused by temperature changes (Figures S7a–S7d in Supporting Information S1). Quantitatively, in Pacific coastal upwelling regions, the cooling effect of $-0.06°C$ month^{-1} induced by changes in ocean advection within the mixed layer of near-coast regions (primarily due to stronger upwelling), accounts for only 9% of the cooling effect of $-0.68°C$ month^{-1} induced by upward transport of colder water induced by Chl shading. In Atlantic coastal upwelling regions, the weaker upwelling contributes to 12% of the warming effect caused by Chl-induced solar absorption.

The simulation of phytoplankton growth in the biogeochemistry model (MEDUSA) is based on the temperature, nutrients and SR availability, influenced by the physical conditions provided by the ocean model (NEMO). Therefore, the variations in ocean physics caused by Chl-induced solar absorption may initiate a feedback effect on Chl concentrations. In Pacific upwelling regions, the stronger upwelling in Case.MED supplies more nutrients to the upper ocean, resulting in increased Chl concentrations in the surface ocean (Figure 2b). Conversely, in Atlantic coastal upwelling regions, weaker upwelling leads to lower Chl concentrations near the coast (Figure 2d) (Messié & Chavez, 2015). However, in the areas away from the Atlantic coast, the penetration of more SR into the subsurface ocean in Case.MED contributes to higher subsurface Chl concentrations (Figure 2d). Overall, the surface Chl maximum in Pacific coastal upwelling regions and subsurface Chl maximum in Atlantic coastal upwelling regions can significantly impact ocean thermal structure and dynamics. These effects, in turn, trigger a positive feedback that reinforces the Chl distribution pattern in each coastal upwelling region (Figures 2a–2d).
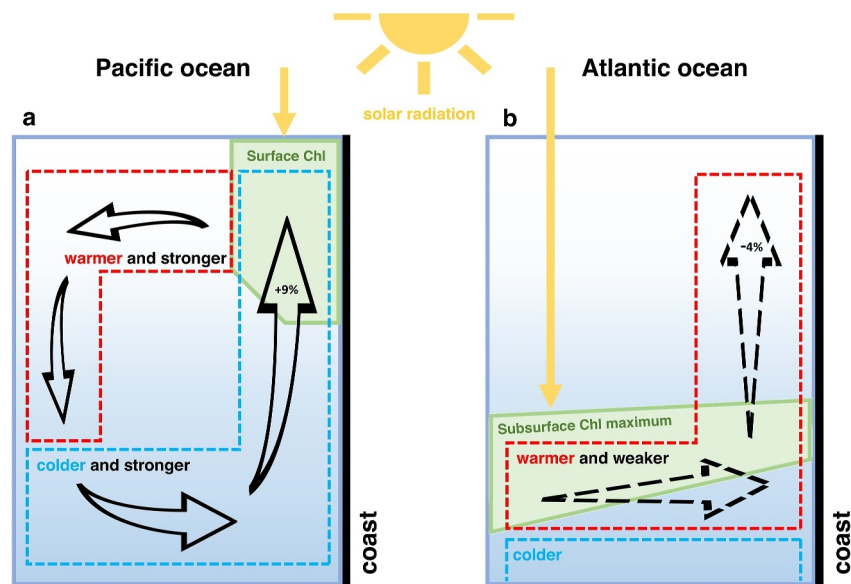
Figure 4. Schematic figure of the oceanic responses to Chl-induced solar absorption in Pacific (a) and Atlantic (b) coastal upwelling regions. Black arrows represent the mean state of ocean currents in coastal upwelling regions, with solid arrows indicating stronger currents and dashed arrows representing weaker currents resulting from enhanced Chl-induced solar absorption. The red dashed boxes and blue dashed boxes indicate warmer and colder temperature zones respectively caused by Chl-induced solar absorption. The percentages inside the arrows quantify the variations in upwelling speed attributed to Chl-induced solar absorption.

Figure 4 summarizes the different mechanisms behind Chl-induced variations in ocean thermal structure and dynamics between Pacific and Atlantic coastal upwelling regions. This discrepancy arises from different Chl distributions in these two regions (green boxes in Figure 4). In Pacific coastal upwelling regions, the high surface Chl concentrations near the coast induce a shading effect in the subsurface ocean that is then upwelled, consequently leading to colder near-surface waters, a more stratified upper ocean and stronger circulation associated with the upwelling (Figure 4a). In Atlantic coastal upwelling regions, the subsurface Chl maximum absorbs SR and leads to a warmer upper ocean and weaker circulation (Figure 4b). This study highlights the importance of considering the spatial distributions of Chl when analyzing its effect on coastal upwelling.

Compared to the impact of Chl-induced solar absorption in equatorial upwelling, which has been shown to significantly influence large-scale circulation (Nakamoto et al., 2001; Shi et al., 2023) and climate variability such as ENSO (Kang et al., 2017; R. H. Zhang et al., 2009), the effect in coastal upwelling regions appears to be more localized. However, the variations in ocean thermal structure driven by Chl in coastal upwelling have the potential to impact stratocumulus clouds in the atmosphere over the upwelling regions and also the climate on a broader scale. SST changes in coastal upwelling regions could alter the lower tropospheric stability, thereby impacting the formation and persistence of oceanic stratocumulus clouds. The response of stratocumulus clouds to SST variations varies widely among models. Some models suggest a decrease in cloud cover (positive feedback), while others indicate an increase (negative feedback) in response to warmer surface in coastal upwelling regions (Brient & Bony, 2012; Qu et al., 2014; M. Zhang & Bretherton, 2008). Nevertheless, it is undeniable that temperature variations driven by Chl-induced solar absorption can influence the formation and equatorward propagation of stratocumulus clouds and subsequently impact the tropical climate (Hu et al., 2008; Yu & Mechoso, 1999).

In this paper, we have shown that the variability in Chl-induced solar absorption has a crucial role in regulating the ocean thermal structure, dynamics, and climate, yet is absent in some physical ocean models and coupled climate models such as UKESM1. Therefore, this biophysical feedback needs to be incorporated into future versions of UKESM and other Earth system models to achieve a more realistic simulation of ocean physics and improve our understanding of climate dynamics.

Data Availability Statement

Model: The NEMO ocean engine is publicly available at Madec and NEMO team (2016), and MEDUSA description can be found at Yool et al. (2013). Model output and the data used for the figures, along with the relevant MATLAB codes, are available at Meng (2024). Data set: Level-3 Mapped Chl-*a* data from MODIS-Aqua ocean color observation are available at NASA OBPG (2022). Software: Model output analysis and visualization are performed using the MATLAB R2021 available at The MathWorks, Inc. (2021), with license (846201) offered by University of East Anglia.

References

Asselot, R., Lunkeit, F., Holden, P. B., & Hense, I. (2021). The relative importance of phytoplankton light absorption and ecosystem complexity in an Earth system model. *Journal of Advances in Modeling Earth Systems*, *13*(5), e2020MS002110. https://doi.org/10.1029/2020MS002110

Brient, F., & Bony, S. (2012). Interpretation of the positive low-cloud feedback predicted by a climate model under global warming. *Climate Dynamics*, *40*(9–10), 2415–2431. https://doi.org/10.1007/s00382-011-1279-7

Chavez, F. P., & Messié, M. (2009). A comparison of eastern boundary upwelling ecosystems. *Progress in Oceanography*, *83*(1–4), 80–96. https://doi.org/10.1016/j.pocean.2009.07.032

Dai, M., Luo, Y. W., Achterberg, E. P., Browning, T. J., Cai, Y., Cao, Z., et al. (2023). Upper ocean biogeochemistry of the oligotrophic north Pacific subtropical gyre: From nutrient sources to carbon export. *Reviews of Geophysics*, *61*(3), e2022RG000800. https://doi.org/10.1029/2022RG000800

Ding, H., Alexander, M. A., & Jacox, M. G. (2021). Role of geostrophic currents in future changes of coastal upwelling in the California current system. *Geophysical Research Letters*, *48*(3), e2020GL090768. https://doi.org/10.1029/2020GL090768

Du, T., Wang, S., Jing, Z., Wu, L., Zhang, C., & Zhang, B. (2024). Future changes in coastal upwelling and biological production in eastern boundary upwelling systems. *Nature Communications*, *15*(1), 6238. https://doi.org/10.1038/s41467-024-50570-z

Echevin, V., Hauschildt, J., Colas, F., Thomsen, S., & Aumont, O. (2021). Impact of chlorophyll shading on the Peruvian upwelling system. *Geophysical Research Letters*, *48*(19), 2021GL094429. https://doi.org/10.1029/2021GL094429

Ferreira, A., Brotas, V., Palma, C., Borges, C., & Brito, A. C. (2021). Assessing phytoplankton bloom phenology in upwelling-influenced regions using ocean color remote sensing. *Remote Sensing*, *13*(4), 1–27. https://doi.org/10.3390/rs13040675

Griffies, S. M., Biastoch, A., Böning, C., Bryan, F., Danabasoglu, G., Chassignet, E. P., et al. (2009). Coordinated ocean-ice reference experiments (COREs). *Ocean Modelling*, *26*(1–2), 1–46. https://doi.org/10.1016/j.ocemod.2008.08.007

Hernandez, O., Jouanno, J., Echevin, V., & Aumont, O. (2017). Modification of sea surface temperature by chlorophyll concentration in the Atlantic upwelling systems. *Journal of Geophysical Research: Oceans*, *122*(7), 5367–5389. https://doi.org/10.1002/2016JC012330

Hilt, M., Auclair, F., Benshila, R., Bordois, L., Capet, X., Debreu, L., et al. (2020). Numerical modelling of hydraulic control, solitary waves and primary instabilities in the strait of Gibraltar. *Ocean Modelling*, *151*, 101642. https://doi.org/10.1016/j.ocemod.2020.101642

Hu, Z. Z., Huang, B., & Pegion, K. (2008). Low cloud errors over the southeastern Atlantic in the NCEP CFS and their association with lower-tropospheric stability and air-sea interaction. *Journal of Geophysical Research*, *113*(D12), D12114. https://doi.org/10.1029/2007JD009514

Huan, Y., Sun, D., Wang, S., Zhang, H., Qiu, Z., Bilal, M., & He, Y. (2021). Remote sensing estimation of phytoplankton absorption associated with size classes in coastal waters. *Ecological Indicators*, *121*, 107198. https://doi.org/10.1016/j.ecolind.2020.107198

Jing, Z., Wang, S., Wu, L., Wang, H., Zhou, S., Sun, B., et al. (2023). Geostrophic flows control future changes of oceanic eastern boundary upwelling. *Nature Climate Change*, *13*, 148–154. https://doi.org/10.1038/s41558-022-01588-y

Jochum, M., Yeager, S., Lindsay, K., Moore, K., & Murtugudde, R. (2010). Quantification of the feedback between phytoplankton and ENSO in the community climate system model. *Journal of Climate*, *23*(11), 2916–2925. https://doi.org/10.1175/2010JCLI3254.1

Kang, X., Zhang, R. H., Gao, C., & Zhu, J. (2017). An improved ENSO simulation by representing chlorophyll-induced climate feedback in the NCAR Community Earth System Model. *Scientific Reports*, *7*(1), 17123. https://doi.org/10.1038/s41598-017-17390-2

Kuhlbrodt, T., Jones, C. G., Sellar, A., Storkey, D., Blockley, E., Stringer, M., et al. (2018). The low-resolution version of HadGEM3 GC3.1: Development and evaluation for global climate. *Journal of Advances in Modeling Earth Systems*, *10*(11), 2865–2888. https://doi.org/10.1029/2018MS001370

Lee, S., Chae, J. Y., Park, J. H., Kim, Y. T., Kang, B., Shin, C. W., & Ha, H. K. (2024). Remote impacts of low-latitude oceanic climate on coastal upwelling in a marginal sea of the northwestern Pacific. *Regional Studies in Marine Science*, *69*, 103344. https://doi.org/10.1016/j.rsma.2023.103344

Lengaigne, M., Menkes, C., Aumont, O., Gorgues, T., Bopp, L., André, J. M., & Madec, G. (2007). Influence of the oceanic biology on the tropical Pacific climate in a coupled general circulation model. *Climate Dynamics*, *28*(5), 503–516. https://doi.org/10.1007/s00382-006-0200-2

Madec, G., & NEMO team. (2016). NEMO ocean engine, version 3.6 stable [ComputationalNotebook]. Note du Pôle de Modélisation de l'Institut Pierre-Simon Laplace. Retrieved from https://zenodo.org/records/3248739

Manizza, M., Quéré, C. L., Watson, A. J., & Buitenhuis, E. T. (2005). Bio-optical feedbacks among phytoplankton, upper ocean physics and sea-ice in a global model. *Geophysical Research Letters*, *32*(5), 1–4. https://doi.org/10.1029/2004GL020778

Manizza, M., Quéré, C. L., Watson, A. J., & Buitenhuis, E. T. (2008). Ocean biogeochemical response to phytoplankton-light feedback in a global model. *Journal of Geophysical Research*, *113*(C10), C10010. https://doi.org/10.1029/2007JC004478

Marlon, L., Mary-Elena, C., Gene, F., Wayne, E., & Chuck, M. (1990). Influence of penetrating solar radiation on the heat budget of the equatorial Pacific ocean. *Nature*, *347*(6293), 543–545. https://doi.org/10.1038/347543a0

Meng, S. (2024). Data for manuscript #2024GL109714 [Dataset]. https://doi.org/10.5281/zenodo.13372292

Mercado, J. M., & Gómez-Jakobsen, F. (2022). Seasonal variability in phytoplankton light absorption properties: Implications for the regional parameterization of the chlorophyll a specific absorption coefficients. *Continental Shelf Research*, *232*, 104614. https://doi.org/10.1016/j.csr.2021.104614

Messié, M., & Chavez, F. P. (2015). Seasonal regulation of primary production in eastern boundary upwelling systems. *Progress in Oceanography*, *134*, 1–18. https://doi.org/10.1016/j.pocean.2014.10.011

Morel, A. (1988). Optical modeling of the upper ocean in relation to its biogenous matter content (case I waters). *Journal of Geophysical Research*, *93*(C9), 10749–10768. https://doi.org/10.1029/jc093ic09p10749

Morel, A., & Berthon, J.-F. B. (1989). Surface pigments, algal biomass profiles, and potential production of the euphotic layer: Relationships reinvestigated in view of remote-sensing applications. *Limnology & Oceanography*, *34*(8), 1545–1562. https://doi.org/10.4319/lo.1989.34.8.1545

Murtugudde, R., Beauchamp, J., Mcclain, C. R., Lewis, M., & Busalacchi, A. J. (2001). Effects of penetrative radiation on the upper tropical ocean circulation. *Journal of Climate*, *15*(5), 470–486. https://doi.org/10.1175/1520-0442(2002)015⟨0470:EOPROT⟩2.0.CO;2

Nakamoto, S., Kumar, S. P., Oberhuber, J. M., Ishizaka, J., Muneyama, K., & Frouin, R. (2001). Response of the equatorial Pacific to chlorophyll pigment in a mixed layer isopycnal ocean general circulation model. *Geophysical Research Letters*, *28*(10), 2021–2024. https://doi.org/10.1029/2000GL012494

NASA Goddard Space Flight Center, Ocean Ecology Laboratory, Ocean Biology Processing Group(OBPG). (2022). Moderate-resolution imaging spectroradiometer (MODIS) aqua data [Dataset]. *NASA OB.DAAC*. https://doi.org/10.5067/AQUA/MODIS/L3M/CHL/2022

Parida, C., Lotliker, A. A., Roy, R., & Vinayachandran, P. N. (2022). Radiant heating rate associated with chlorophyll dynamics in upper ocean of southern bay of Bengal: A case study during bay of Bengal boundary layer experiment. *Deep-Sea Research Part II Topical Studies in Oceanography*, *196*, 105026. https://doi.org/10.1016/j.dsr2.2022.105026

Park, J. Y., Kug, J. S., Bader, J., Rolph, R., & Kwon, M. (2015). Amplified Arctic warming by phytoplankton under greenhouse warming. *Proceedings of the National Academy of Sciences of the United States of America*, *112*(19), 5921–5926. https://doi.org/10.1073/pnas.1416884112

Park, J. Y., Kug, J. S., & Park, Y. G. (2014). An exploratory modeling study on bio-physical processes associated with ENSO. *Progress in Oceanography*, *124*, 28–41. https://doi.org/10.1016/j.pocean.2014.03.013

Patil, P. A., Adhikari, A., & Menon, H. B. (2023). Bio-optical complexity and radiant heating rates in the coastal waters of eastern Arabian Sea. *Science of the Total Environment*, *884*, 163838. https://doi.org/10.1016/j.scitotenv.2023.163838

Patti, B., Guisande, C., Vergara, A. R., Riveiro, I., Maneiro, I., Barreiro, A., et al. (2008). Factors responsible for the differences in satellite-based chlorophyll a concentration between the major global upwelling areas. Estuarine. *Coastal and Shelf Science*, *76*(4), 775–786. https://doi.org/10.1016/j.ecss.2007.08.005

Qu, X., Hall, A., Klein, S. A., & Caldwell, P. M. (2014). On the spread of changes in marine low cloud cover in climate model simulations of the 21st century. *Climate Dynamics*, *42*(9–10), 2603–2626. https://doi.org/10.1007/s00382-013-1945-z

Richter, I. (2015). Climate model biases in the eastern tropical oceans: Causes, impacts and ways forward. *Wiley Interdisciplinary Reviews: Climate Change*, *6*(3), 345–358. https://doi.org/10.1002/wcc.338

Sellar, A. A., Jones, C. G., Mulcahy, J. P., Tang, Y., Yool, A., Wiltshire, A., et al. (2019). UKESM1: Description and evaluation of the U.K. Earth system Model. *Journal of Advances in Modeling Earth Systems*, *11*(12), 4513–4558. https://doi.org/10.1029/2019MS001739

Shi, Q., Zhang, R. H., & Tian, F. (2023). Impact of the deep chlorophyll maximum in the equatorial Pacific as revealed in a coupled ocean GCM-ecosystem model. *Journal of Geophysical Research: Oceans*, *128*(4), e2022JC018631. https://doi.org/10.1029/2022JC018631

Sweeney, C., Gnanadesikan, A., Griffies, S. M., Harrison, M. J., Rosati, A. J., & Samuels, B. L. (2005). Impacts of shortwave penetration depth on large-scale ocean circulation and heat transport. *Journal of Physical Oceanography*, *35*(6), 1103–1119. https://doi.org/10.1175/JPO2740.1

The MathWorks, Inc. (2021). MATLAB release r2021a [Software]. https://www.mathworks.com/products/matlab.html

Tian, F., Zhang, R. H., Wang, X., & Zhi, H. (2021). Rectified effects of interannual chlorophyll variability on the tropical Pacific climate revealed by a hybrid coupled physics-biology model. *Journal of Geophysical Research: Oceans*, *126*(6), e2021JC017263. https://doi.org/10.1029/2021JC017263

Timmermann, A., & Jin, F. F. (2002). Phytoplankton influences on tropical climate. *Geophysical Research Letters*, *29*(23), 2104. https://doi.org/10.1029/2002GL015434

Wood, R. (2012). Stratocumulus clouds. *Monthly Weather Review*, *140*(8), 2373–2423. https://doi.org/10.1175/MWR-D-11-00121.1

Yasunaka, S., Ono, T., Sasaoka, K., & Sato, K. (2022). Global distribution and variability of subsurface chlorophyll a concentrations. *Ocean Science*, *18*(1), 255–268. https://doi.org/10.5194/os-18-255-2022

Yool, A., Palmiéri, J., Jones, C. G., Mora, L. D., Kuhlbrodt, T., Popova, E. E., et al. (2021). Evaluating the physical and biogeochemical state of the global ocean component of UKESM1 in CMIP6 historical simulations. *Geoscientific Model Development*, *14*(6), 3437–3472. https://doi.org/10.5194/gmd-14-3437-2021

Yool, A., Popova, E. E., & Anderson, T. R. (2013). MEDUSA-2.0: An intermediate complexity biogeochemical model of the marine carbon cycle for climate change and ocean acidification studies. *Geoscientific Model Development*, *6*(5), 1767–1811. https://doi.org/10.5194/gmd-6-1767-2013

Yu, J.-Y., & Mechoso, C. R. (1999). Links between annual variations of Peruvian stratocumulus clouds and of SST in the eastern equatorial Pacific. *Journal of Climate*, *12*(11), 3305–3318. https://doi.org/10.1175/1520-0442(1999)012⟨3305:LBAVOP⟩2.0.CO;2

Zhang, M., & Bretherton, C. (2008). Mechanisms of low cloud-climate feedback in idealized single-column simulations with the Community Atmospheric Model, version 3 (CAM3). *Journal of Climate*, *21*(18), 4859–4878. https://doi.org/10.1175/2008JCLI2237.1

Zhang, R. H., Busalacchi, A. J., Wang, X., Ballabrera-Poy, J., Murtugudde, R. G., Hackert, E. C., & Chen, D. (2009). Role of ocean biology-induced climate feedback in the modulation of El Niño-Southern Oscillation. *Geophysical Research Letters*, *36*(3), 2008GL036568. https://doi.org/10.1029/2008GL036568

Zhang, R. H., Tian, F., & Wang, X. (2018). A new hybrid coupled model of atmosphere, ocean physics, and ocean biogeochemistry to represent biogeophysical feedback effects in the tropical Pacific. *Journal of Advances in Modeling Earth Systems*, *10*(8), 1901–1923. https://doi.org/10.1029/2017MS001250

Zhang, R. H., Tian, F., Zhi, H., & Kang, X. (2019). Observed structural relationships between ocean chlorophyll variability and its heating effects on the ENSO. *Climate Dynamics*, *53*(9–10), 5165–5186. https://doi.org/10.1007/s00382-019-04844-8